Applied Catalysis B: Environmental 162 (2015) 245–251

Contents lists available at ScienceDirect

Applied Catalysis B: Environmental

journal homepage: www.elsevier.com/locate/apcatb

NH_2-mediated indium metal–organic framework as a novel visible-light-driven photocatalyst for reduction of the aqueous Cr(VI)

Ruowen Liang, Lijuan Shen, Fenfen Jing, Weiming Wu, Na Qin, Rui Lin, Ling Wu*

State Key Laboratory of Photocatalysis on Energy and Environment, Fuzhou University, Fuzhou 350002, PR China

ARTICLE INFO

Article history:
Received 9 April 2014
Received in revised form 20 June 2014
Accepted 26 June 2014
Available online 5 July 2014

Keywords:
MOFs
NH_2-mediated
Photocatalysis
Visible light
Cr(VI) reduction

ABSTRACT

Metal–organic framework In-benzenedicarboxylate (MIL-68(In)) and its derivative (In-2-NH_2-benzenedicarboxylate, MIL-68(In)-NH_2) were prepared via a simple solvothermal method. Powder X-ray diffraction (XRD) confirmed the isoreticular nature of MIL-68(In) and MIL-68(In)-NH_2, while Fourier transformed infrared spectra (FTIR) proved the effective presence of amino group. Moreover, combined with UV–vis diffuse reflectance spectra (DRS) analysis, it was revealed MIL-68(In)-NH_2 shown an extra absorption band in the visible light region with the absorption edge extending to around 440 nm. Importantly, MIL-68(In)-NH_2 was proved to perform as an efficient visible-light-driven photocatalyst with considerable activity and stability for the reduction of Cr(VI), which could be attributed to its relatively high CB based on the result of Mott–Schottky experiment. Further experimental results revealed that the addition of hole scavenger and pH value of the reaction solution played important roles in the photocatalytic reduction of Cr(VI). Finally, a possible reaction mechanism had also been investigated in detail.

1. Introduction

Hexavalent chromium (Cr(VI)) is a frequent contaminant in wastewater arising from industrial processes such as leather tanning, paint making, and so on. Its removal from wastewater is of crucial importance because it is harmful to biological systems and can easily get into the food chains [1]. One of the most preferred methods to treat Cr(VI) in wastewater is the transformation of Cr(VI) to Cr(III). The Cr(III) is considered nontoxic and is an essential trace metal in human nutrition. Furthermore, it can be precipitated and removed as a solid waste. The common methods currently adopted to remove Cr(VI) from wastewater including precipitation, ion exchange and photocatalysis reduction [2–4]. Among these methods, photocatalysis is a promising technique since it achieves the one-pot removal of Cr(VI) by utilizing sunlight. It has been reported that TiO_2, ZnO, and $La_2Ti_2O_7$ can photocatalytic reduce Cr(VI) to Cr(III) [5–7]. However, they only be activated under UV light irradiation, which greatly restrict their applied extensively. In order to efficiently utilize the sunlight, it is necessary to develop novel visible-light-driven photocatalysts for the reduction of Cr(VI).

Metal–organic frameworks (MOFs) are a class of inorganic–organic hybrid materials with infinite three-dimensional networks [8–10]. Their intriguing aesthetic structures and outstanding properties such as high pore volume, high specific surface area, structural adaptivity and flexibility have led to the successful application of MOFs in gas storage and capture, sensor devices, drug release, and catalysis [11–15]. Recently, a new, burgeoning direction in the field of MOFs is their use as photocatalysts [16,17]. Compared with the traditional photocatalysts, the superiority of MOFs is that the band gap in MOFs systems is closely related to the HOMO–LUMO gap which allow for fine-tuning and rational design of these photocatalysts at the molecular level [18–21]. García and his co-workers have studied MOF-5 as a semiconductor for photodegradation of phenol in aqueous solutions and water stable Zr–benzenedicarboxylate MOF as photocatalysts for hydrogen generation [22–24]. However, because of the lack of visible light response, these materials would show limited efficiency under solar illumination. An opportunity to tune these optical properties lies in the modification of the organic linkers, yielding an elevated visible light response. In this context, NH_2-mediated MIL-125(Ti) has been studied and shown activity for photocatalytic CO_2 reduction and hydrogen generation [25,26]. Our recent studies have mainly focused on syntheses and modification of NH_2-mediated zirconium metal–organic framework, which exhibited excellent photocatalytic activity and

* Corresponding author. Tel.: +86 591 83779362; fax: +86 591 83779105.
E-mail addresses: Wuling@fzu.edu.cn, 2307422493@qq.com (L. Wu).

http://dx.doi.org/10.1016/j.apcatb.2014.06.049
0926-3373/

stability [28–31]. Multiple studies have testified the photocatalytic activity of titanium and zirconium based MOFs [25–27]. However, to the best of our knowledge, no attention has ever been paid to study the photocatalytic properties of In-containing MOFs to date.

MIL-68(In) was chosen as the target of the research owing to its high thermal stability, adjustability and photoresponsiveness [32]. Besides, considering that MIL-68(In) can only be photoexcited under ultraviolet (UV) light irradiation, it is unfavorable to fully utilize the solar energy. Thus, we report a targeted photoactive catalyst amino-modified MIL-68(In) (MIL-68(In)-NH_2), which photoabsorption edge could be efficiently shifted to visible light region by simply introducing the amino group to organic ligand. Moreover, the photocatalytic performance of MIL-68(In)-NH_2 photocatalyst on the photocatalytic reduction of Cr(VI) to Cr(III) was investigated in detail, including the effects of the addition of hole scavenger, pH value, the stability of the catalyst and a mechanism was also proposed to explained the photocatalytic reduction of Cr(VI) over MIL-68(In)-NH_2. It is expected that our current work could provide guided information for tuning their photoabsorption and widen the application range of the MOFs.

2. Experimental

2.1. Preparation of photocatalysts

All reagents and solvents were used as received from commercial suppliers without further purification. 1,4-benzenedicarboxylic acid (H_2BDC), and 2-aminoterephthalic acid (H_2ATA) were obtained from Alfa Aesar China Co., Ltd. (Tianjin, China). indium nitrate hydrate ($In(NO_3)_3{\cdot}xH_2O$), *N*,*N*-dimethylformamide (DMF), ethanol, ammonium oxalate, and ammonium oxalate were supplied by Sinopharm Chemical Reagent Co., Ltd. (Shanghai, China).

2.1.1. Synthesis of MIL-68(In) sample

MIL-68(In) was prepared via a modified method reported previous [31]. In a typical synthesis, 1.05 mmol of $In(NO_3)_3{\cdot}xH_2O$, 1.20 mmol of 1,4-benzenedicarboxylic acid were dissolved 12.4 mL of DMF in a 30 mL Teflon liner. After stirred for 30 min (500 r min^{-1}), the Teflon liner was sealed in a stainless steel autoclave and maintained at 100 °C for 48 h. The resulting white powder consisted of elongated needlelike crystallites was collected.

2.1.2. Synthesis of MIL-68(In)-NH_2 sample

MIL-68(In)-NH_2 was synthesized by a solvothermal method [33]. Typical, 3.84 mmol of $In(NO_3)_3{\cdot}xH_2O$, 1.29 mmol of 2-aminoterephthalic acid were dissolved 12.4 mL of DMF in a 30 mL Teflon liner. After stirred for 30 min (500 r min^{-1}), the Teflon liner was sealed in a stainless steel autoclave and maintained at 125 °C for 5 h. Light yellow MIL-68(In)-NH_2 powder was collected.

Before using the samples for the photocatalytic reactions, an activation process was performed on all bulk samples. In order to remove the guest molecules in the pores, the as-synthesized sample was stirred in anhydrous methanol for three days. Then, the samples were filtered and were dried under vacuum at 100 °C for 12 h.

2.2. Characterizations

XRD patterns were carried on a Bruker D8 Advance X-ray diffractometer operated at 40 kV and 40 mA with Ni-filtered Cu *K*a irradiation (λ = 0.15406 nm). The data were recorded in the 2θ range of 4–30°. UV–vis diffuse reflectance spectra (UV–vis DRS) were obtained by a UV–vis spectrophotometer (Varian Cary 500) and the data were converted to Kubelka–Munk functions. Barium sulfate was used as a reference. FT-infrared (FT-IR) spectra were carried out on a Nicolet 670 Fourier transform infrared spectrometer. FT-IR spectra of pure samples were collected with KBr pellets in the 500–4000 cm^{-1} region. The spectra were registered after accumulation of 32 scans and a resolution of 4 cm^{-1}. The Brunauer–Emmett–Teller (BET) surface area was measured with an ASAP2020M apparatus (Micromeritics Instrument Corp., USA). Before the test, the samples were degassed in vacuum at 180 °C for 12 h. The nitrogen adsorption and desorption isotherms were measured at 77 K. The zeta potentials (ξ) of sample were determined by dynamic light scattering analysis (Zeta sizer 3000HSA) at a room temperature of 25 °C. Cyclic voltammograms (CVs) were recorded by a CHI 810B electrochemical workstation (Chenhua, Shanghai, China). A conventional three-electrode system was used, with a glassy carbon electrode as the working electrode, an Ag/AgCl (3 M KCl) electrode as the reference one and a Pt foil as the auxiliary one. The concentration of indium in the supernate was detected by the Ultima2 ICP optical emission spectrometer. Mott–Schottky measurement was obtained at a Zenuium electrochemical workstation (Zahner Co.). The measurement was performed in a conventional three electrode cell, using Pt plate and Ag/AgCl electrode as the counter electrode and reference electrode, respectively. The working electrode was prepared on a fluorinedoped tin oxide (FTO) glass. Furthermore, 0.1 M of Na_2SO_4 solution was used as electrolyte. The photocurrent measurements were conducted with a BAS Epsilon workstation. A 300 W Xe lamp (PLS-SXE 300, Beijing Perfectlight Co. Ltd) with a 420 nm cut-off filter was used as a light source. Moreover, the total organic carbon (TOC) values of the organic pollutants aqueous solutions were detected by a Shimadzu TOC-V_{CPH} total organic carbon analyzer.

2.3. Evaluation of photocatalytic activity

The photocatalytic reduction of aqueous Cr(VI) to Cr(III) was carried out at 30 °C in a 100 mL quartz reactor containing 40 mg photocatalyst and 40 mL 20 ppm Cr(VI) aqueous solution. The pH values of reaction solutions were adjusted with H_2SO_4 or NaOH. Without any additives, the pH value of the suspension was about 6. Nitrogen was then purged through the system, followed by the introduction of the organic compound (5 mg or 200 μL) into the suspension. After being stirred for 1 h to reach adsorption-desorption equilibrium, the suspensions were irradiated by a 300 W Xe lamp (PLS-SXE 300, Beijing Perfectlight Co. Ltd) with 420 nm cut-off filter. During illumination, about 2 mL of suspension was taken from the reactor at a scheduled interval and centrifuged to separate the photocatalyst. The Cr(VI) content in the supernatant solution was determined colorimetrically at 540 nm using the diphenylcarbazide method (DPC) with a Cary 50 UV–vis spectrophotometer (Varian Co.) [34]. The measured absorbance intensities at different illumination times were transformed to the reduction ratio of Cr(VI), which is calculated using the following expression:

$$\text{Reduction ratio of Cr(VI)} = \frac{(C_0 - C_t)}{C_0} \times 100\%$$

where C_0 and C_t are the absorbance intensities when illuminated for 0 and t min, respectively.

3. Results and discussion

3.1. Characterizations

XRD patterns of the as-prepared samples are shown in Fig. 1. The diffraction peaks of the MIL-68(In) and MIL-68(In)-NH_2 are similar, which verifies the isostructural relationship between the samples [32,33]. This further reveals that the presence of NH_2 group in the organic linker does not influence the structure of MIL-68(In). The FTIR spectra of MIL-68(In)-NH_2 (see Fig. 2) can confirm the

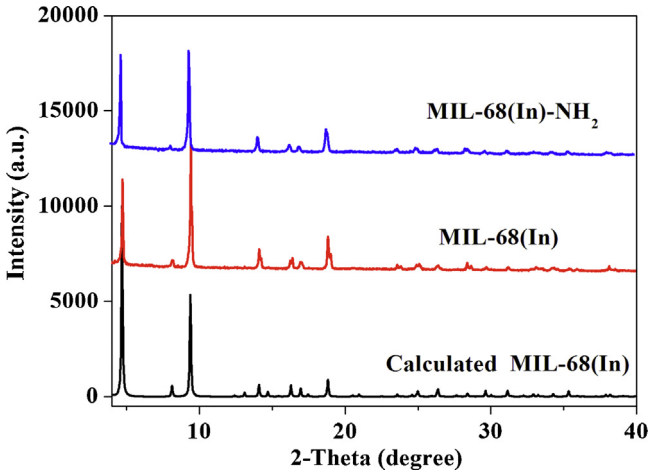

Fig. 1. XRD patterns of samples.

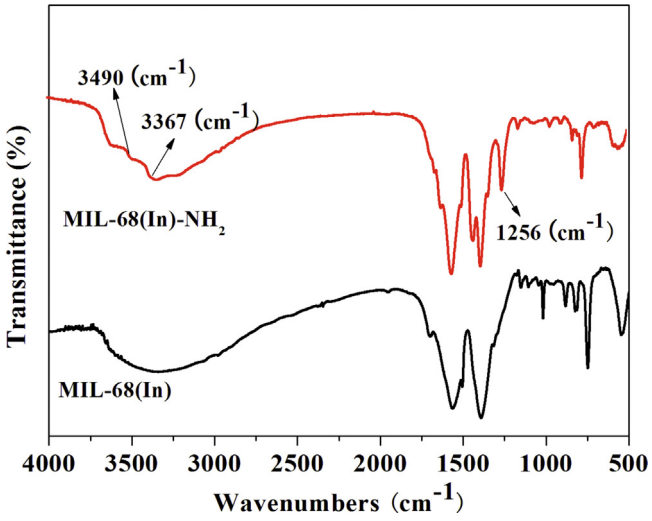

Fig. 2. IR spectra of samples.

introducing of the amino group (-NH_2) to the organic ligand. The bands at 3490 and 3367 cm^{-1} attribute to the symmetric and asymmetric stretching of primary amines. Furthermore, the peak at 1256 cm^{-1} can be ascribed to the stretching vibration of N—C. The BET surface area and porous structure of MIL-68(In)-NH_2 have also been investigated in this work (see Fig. S1). The results show that the BET surface area is 674.0 $m^2 g^{-1}$ for MIL-68(In)-NH_2, which is similar to that of MIL-68(In) (681.4 $m^2 g^{-1}$).

As shown in Fig. 3, UV–vis DRS spectra of the as-prepared samples reveal that the samples present semiconductor properties. The characteristic absorption peak at about 360–380 nm in H_2ATA and MIL-68(In)-NH_2 can be ascribed to the n–π* transition of the electron lone pair of the amino group in ATA [35]. However, the blue shift of the absorption bands of MIL-68(In)-NH_2 (360 nm) versus that in free ligand (390 nm) could be attributed to the perturbation of the transitions by the metal center in the MOFs [36]. Moreover, MIL-68(In)-NH_2 shows an absorption edge at 440 nm, corresponding to a band gap of 2.82 eV, whereas MIL-68(In) shows a band gap of 3.88 eV. The result further indicates that the photoabsorption edge of MIL-68(In)-NH_2 could be shifted to the visible light region by simply introducing the amino group (—NH_2) to the organic ligand, which conforms with the color changing from white to yellow (inset in Fig. 3).

In order to better understand the intrinsic electronic properties of MIL-68(In) and MIL-68(In)-NH_2, Mott–Sckottky measurements

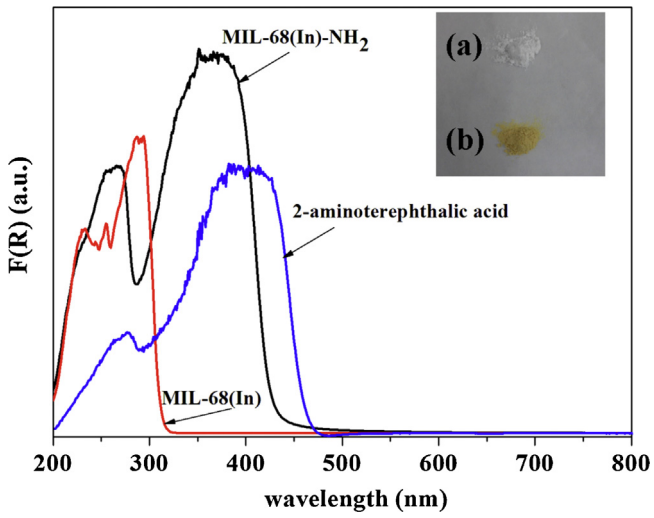

Fig. 3. UV–vis spectra of 2-aminoterephthalic acid, MIL-68(In) and MIL-68(In)-NH_2, the inset are the photographs of (a) MIL-68(In) and (b) MIL-68(In)-NH_2.

were also performed in darkness. As shown in Fig. 4(a), the flat-band potential of MIL-68(In)-NH_2 determined from Mott–Schottky plots is ca. −0.92 V versus Ag/AgCl at pH = 6.8, corresponding to a potential of −0.72 V versus NHE at pH = 6.8. Furthermore, MIL-68(In)-NH_2 shows the characteristic behavior of an n-type semiconductor because of the positive slope of the linear plots [37]. For n-type semiconductors, the conduction bands are very close to their flat-band potentials [38]. Therefore, the redox potential of conduction band (CB) of MIL-68(In)-NH_2 is −0.72 V versus NHE at pH = 6.8, which is more negative than the Cr(VI)/Cr(III) potential (+0.51 V, pH = 6.8) [39]. It is thermodynamically permissible for the transformation of photogenerated electrons to the Cr(VI) to produce the Cr(III). As shown in Fig. 4(b), the potential of the CB of MIL-68(In)-NH_2 is the same as that of MIL-68(In). It indicates that the introduction of the amino group reduced the redox potential of valence band (VB) of MIL-68(In)-NH_2. As a result, the photoabsorption edge of MIL-68(In)-NH_2 shifts to the visible light region. Furthermore, as shown in Fig. 4(c), a stable and strong short circuit photocurrent response has been observed over the MIL-68(In)-NH_2 photoelectrode under visible light irradiation. However, no obvious circuit photocurrent has been detected for MIL-68(In), which is consistent with the UV–vis DRS results.

3.2. Reduction of Cr(VI)

Control experiments were first carried out to demonstrate the photocatalytic nature of the reaction. Taking a view of the overall activities from Fig. 5, it can be found that no significant reaction of Cr(VI) is observed in the dark or in the absence of MIL-68(In)-NH_2. And the photocatalytic catalytic of MIL-68(In) can be negligible under the same condition. These results indicate that the photoabsorption edge of MIL-68(In)-NH_2 could be shifted to the visible light region by simply introducing the amino group, and MIL-68(In)-NH_2 shows photocatalytic activity for the Cr(VI) reduce under visible light irradiation.

To obtain the optimum reaction condition, controlled experiments have been carried out with addition of different hole scavengers (such as ethanol, ammonium formate and ammonium oxalate) at pH = 2. As shown in Fig. 6, the addition of the hole scavengers can improve the photocatalytic activity of MIL-68(In)-NH_2 for the reduce of Cr(VI). Compared to other hole scavengers, ethanol is found as the most efficient hole scavenger for the reduction of Cr(VI) over MIL-68(In)-NH_2. It is observed that the MIL-68(In)-NH_2-ethanol system exhibits the highest reduction ratio (97%),

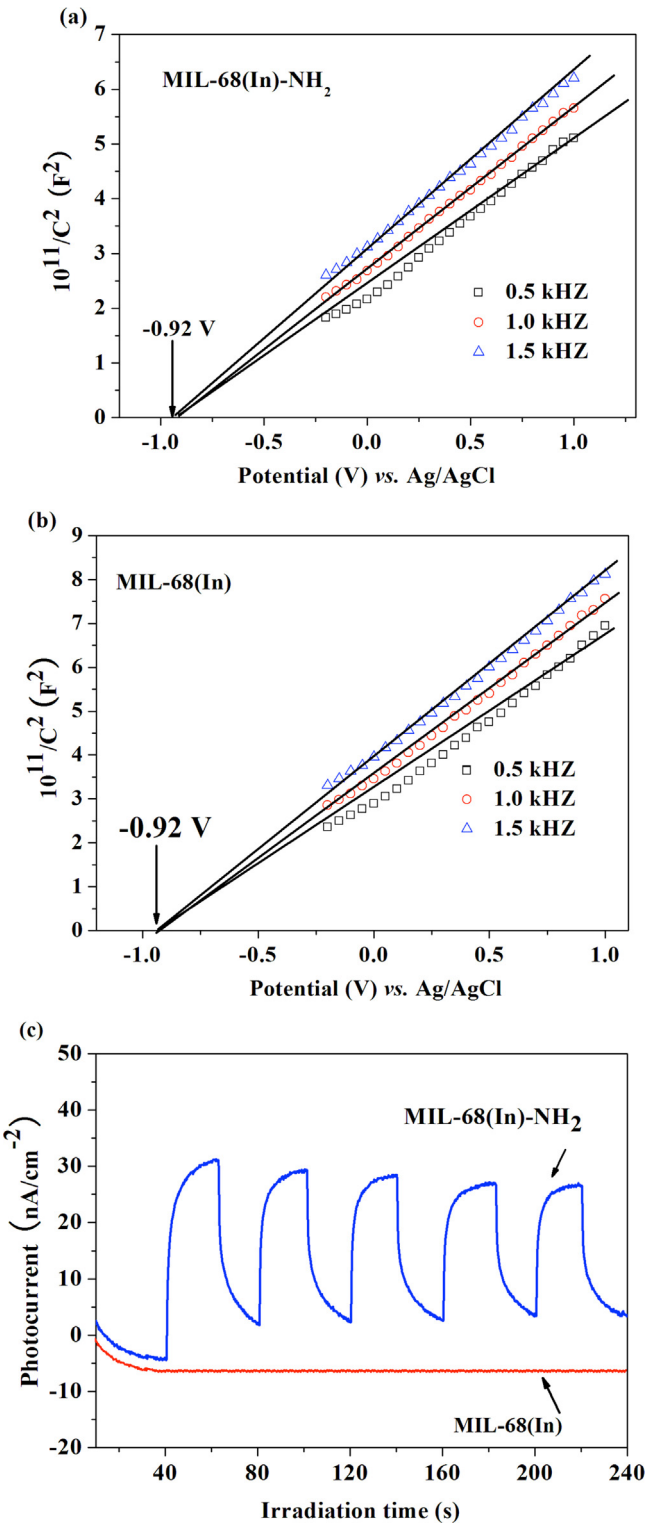

Fig. 4. Typical Mott–Schottky plots of (a) MIL-68(In)-NH_2, (b) MIL-68(In), (c) transient photocurrent response of MIL-68(In)-NH_2 and MIL-68(In) in 0.2 M Na_2SO_4 aqueous solution.

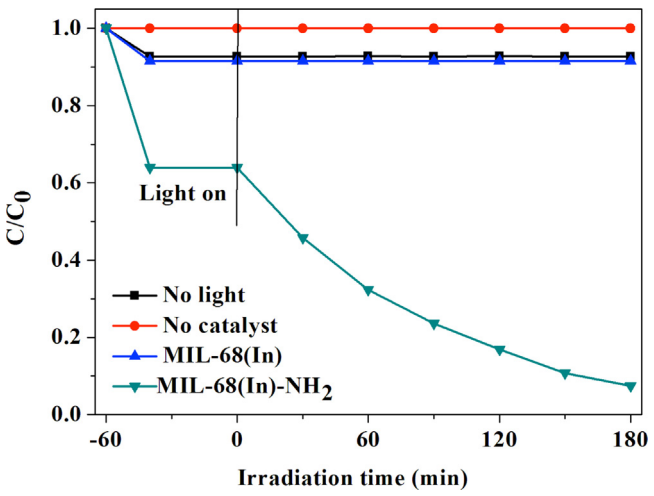

Fig. 5. Photocatalytic reduction of aqueous Cr(VI) under different conditions.

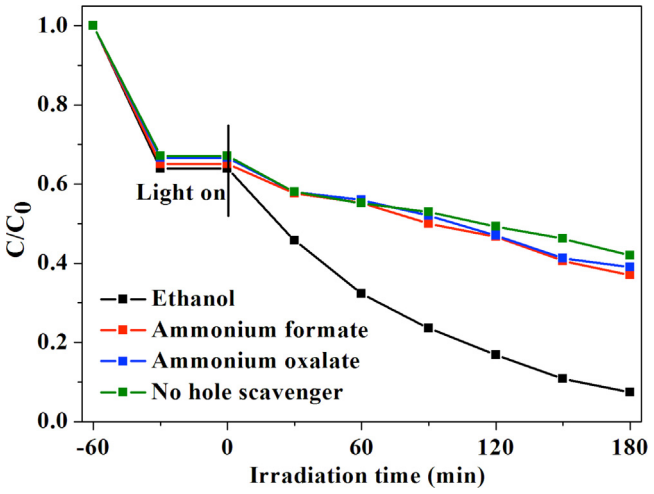

Fig. 6. Photocatalytic activities of MIL-68(In)-NH_2 for the reduction of aqueous Cr(VI) in the presence of various hole scavengers.

which is about 2.25 and 2.10 times higher than that of ammonium oxalate (43%) and ammonium formate (46%), respectively. However, without any additives, the reduction ratio of pure photocatalysis is very slow after 180 min of the visible light irradiation (28%). It is well-known that an effective hole scavenger has to be able to adsorb on the catalyst surface as well as can be mineralized easily in the reaction system [40,41]. The reason for ethanol being the most efficiently hole scavenger could be due to its ability to adsorb on the surface of MIL-68(In)-NH_2. Moreover, ethanol is capable of forming reducing radicals, which can capture photoinduced holes of MIL-68(In)-NH_2. Thus, more electrons can escape from the pair recombination and are available to reduce Cr(VI). Furthermore, Cr(VI) is often discharged together with hazardous organics from industrial wastewater. It is also possible that MIL-68(In)-NH_2 could perform photooxidation of hazardous organics and photoreduction of Cr(VI) together by individually consuming photoelectrons and holes, which makes it a potential candidate for industrial wastewater treatment.

A previous study reported that the reduction rate of aqueous Cr(VI) over photocatalyst was greatly influenced by the pH value of the reaction system [2]. The temporal concentration variation of Cr(VI) reduction by MIL-68(In)-NH_2 at different pH values is shown in Fig. 7. It can be seen that the reduction ratio can be increased rapidly by the decreasing the pH values (28%, 50%, 65% and 97% at pH = 8, 6, 4 and 2, respectively). Simultaneously, the adsorptivity of Cr(VI) over MIL-68(In)-NH_2 increases with the decreasing of the pH value. In order to explore the reason for this phenomenon, the surface zeta potential versus pH for MIL-68(In)-NH_2 was performed. The isoelectric point of MIL-68(In)-NH_2 is determined to be 4.8 (see Fig. S2). When the pH value is below 4.8, the zeta potential of the MIL-68(In)-NH_2 is positive. Therefore, the surface of catalyst can

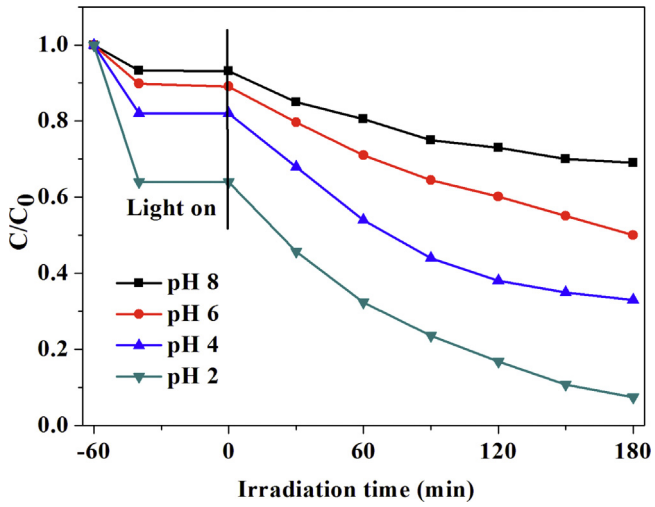

Fig. 7. Photocatalytic activities of MIL-68(In)-NH_2 for the reduction of aqueous Cr(VI) at different pH values.

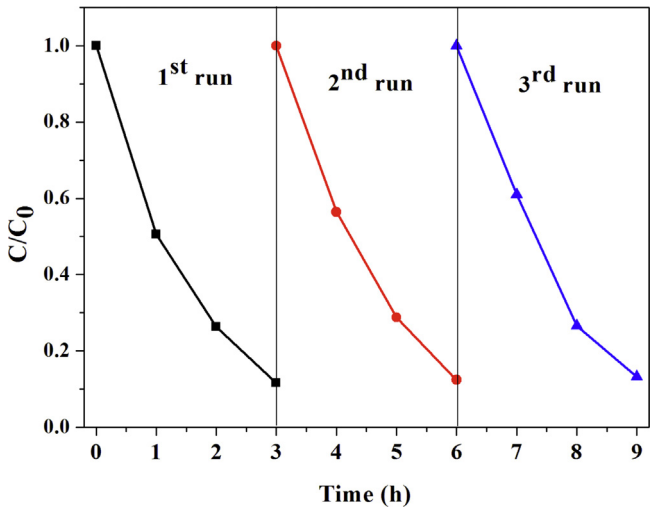

Fig. 8. Reusability of MIL-68(In)-NH_2 for the photocatalytic reduction of Cr(VI). Reaction conditions: 40 mg photocatalyst, 40 mL of 20 ppm Cr(VI), 200 μL ethanol, reaction temperature 30 °C, pH = 2.

be expected to provide better adsorption performance for $Cr_2O_7^{2-}$ anionic. On the other hand, in basic media, the negative charge on MIL-68(In)-NH_2 would electrostatically repel the CrO_4^{2-} anions [42]. Moreover, when the pH value is above 6, Cr(III) will be precipitated on the surface of the photocatalyst as $Cr(OH)_3$ and the activity sites are covered with the precipitation, so the photocatalytic activity decreases.

Furthermore, the reusability and stability of MIL-68(In)-NH_2 for reduction of aqueous Cr(VI) is investigated. In our work, photocatalyst was simply recovered by filtration, washed with 1 mol/L HNO_3 aqueous solution and deionized water, dried in vacuum at 100 °C for 4 h. As shown in Fig. 8, no significant loss of photocatalytic activities after three cycles. XRD and FTIR results (see Fig. 9) reveal that the MIL-68(In)-NH_2 structure were maintained even after the three cycles of the reaction. Moreover, the ICP optical emission spectrometer was applied to analyze the concentration of In(III) during the reaction (see Table S1). As can be observed, there is almost no In(III) ions leaching from the MIL-68(In)-NH_2 during the reaction. In addition, to better understand the photochemical stability of MIL-68(In)-NH_2, cyclic voltammetry measurement was also performed. As shown in Fig. S3, no obvious responses are observed in the ethanol system (curve a), which indicated that the oxidation peak current on ethanol can be negligible under the same condition. Then, 5 μL of MIL-68(In)-NH_2 suspension was decorated onto a glassy carbon electrode (GCE) and dried in air as working electrode called MOF/GCE. For MOF/GCE, a remarkable oxidation peak at about 1.5 V is observed (the CB of MIL-68(In)-NH_2, curve b). However, after injecting 25 μL of ethanol into this system, the peak displays a slight shift toward the negative potential, and the oxidation peak current decrease significantly (curve c). Evidently, the more negative oxidation potential and the large decreased peak current clearly demonstrate that the addition of ethanol could restrain the oxidation of catalyst effectively. Combining the results of XRD, FTIR, ICP and CV, it can be concluded that the MIL-68(In)-NH_2 shows good catalytic reusability and stability in this reaction process.

3.3. Mechanism for the reduction of Cr(VI)

Based on the experimental results, a probable mechanism for the reduction of Cr(VI) over MIL-68(In)-NH_2 has been proposed (see Fig. 10). In this process, the indium–oxygen clusters within MIL-68(In)-NH_2 can behave as quantum dots surrounded by terephthalate ligands with the NH_2 groups performing as auxochromic group, these terephthalate ligands can act as antennae absorbing light and they are able to efficiently transfer the energy to the inorganic indium–oxygen clusters part. Upon light irradiation ($h\nu \geq E_{bg}$), electron excitation takes place in MIL-68(In)-NH_2. The electrons on the CB composed of O, C and N 2p orbitals jump to

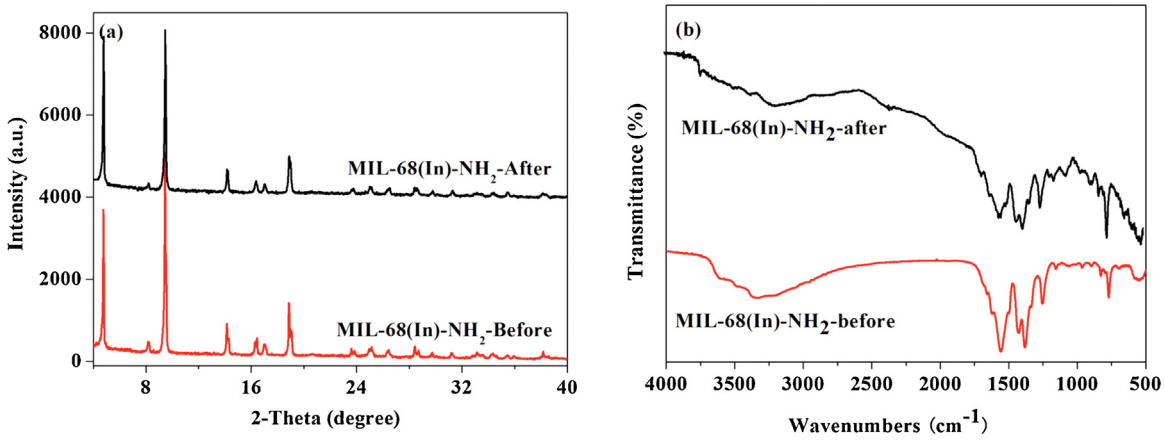

Fig. 9. (a) XRD patterns and (b) FTIR spectra of MIL-68(In)-NH_2 before and after the catalytic reaction.

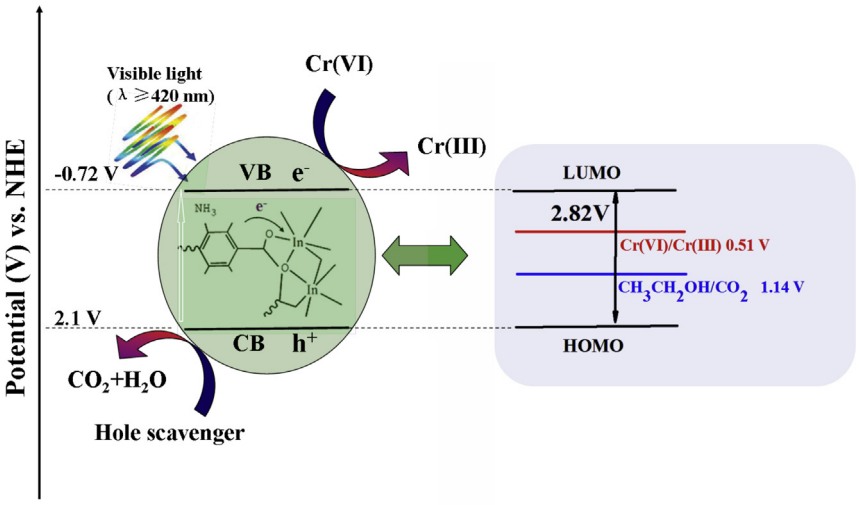

Fig. 10. A schematic illustration of photocatalytic reduction Cr(VI) over MIL-68(In)-NH_2 under visible light irradiation.

the VB, and transfer to Cr(VI) adsorbed on the metal sites to form Cr(III), while the photogenerated holes oxidize the hole scavengers adsorbed on the amine sites to form CO_2 and H_2O (see Fig. S4). Based on the above result, the redox process is always outlined as follows:

$$\text{MIL} - 68(\text{In}) - \text{NH}_2 \xrightarrow{h\nu \geq E_{bg}} \text{MIL} - 68(\text{In}) - \text{NH}_2(h^+ + e^-) \quad (1)$$

$$14H^+ + Cr_2O_7^{2-} + 6e^- \rightarrow 2Cr^{3+} + 7H_2O \quad (2)$$

$$h^+ + CH_3CH_2OH \rightarrow CH_3CH_2OH\bullet + H_2O \rightarrow CO_2 + H_2O + \text{mineral} + \text{acids} \quad (3)$$

4. Conclusions

In summary, the photocatalytic reduction of Cr(VI) to Cr(III) under visible light irradiation is for the first time realized over a photoactive In-containing MOF, MIL-68(In)-NH_2. The photoabsorption edge of MIL-68(In)-NH_2 could be shifted to the visible light region by simply introducing the amino group ($-NH_2$) on the organic ligand. The experimental results indicate that the addition of ethanol enhanced the photocatalytic reduction of Cr(VI) due to its ability to adsorb on the catalyst surface as well as can be mineralized easily in the reaction system. Furthermore, the pH value of the aqueous solution is crucial to the adsorption of Cr(VI) possibly because the presence of various Cr(VI) species and the surface charge of MIL-68(In)-NH_2 are highly pH-dependent. It is hoped that our current work could widen the application range of the MOFs as well as provide a simple and effective method for reduction of Cr(VI) using In-containing MOF as a novel photocatalyst under visible light irradiation.

Acknowledgements

This work was supported by the National Natural Science Foundation of China (21273036 and 21177024) and National Key Basic Research Program of China (Supported by the China Ministry of Science and Technology National 973 Project, 2014CB239303).

Appendix A. Supplementary data

Supplementary data associated with this article can be found, in the online version, at http://dx.doi.org/10.1016/j.apcatb.2014.06.049.

References

[1] M. Owlad, M.K. Aroua, W.A.W. Daud, S. Baroutian, Water, Air, Soil Pollut. 200 (2008) 59–77.
[2] Y. Ku, I.L. Jung, Water Res. 35 (2001) 135–142.
[3] P. Mohapatra, S. Samantaray, K.M. Parida, J. Photochem. Photobiol. A: Chem. 170 (2005) 189–194.
[4] H.B. Yu, S. Chen, X. Quan, H.M. Zhao, Y.B. Zhang, Environ. Sci. Technol. 42 (2008) 3791–3796.
[5] L.B. Khalil, W.E. Mourad, M.W. Rophael, Appl. Catal., B: Environ. 17 (1998) 267–273.
[6] E. Selli, A. De Giorgi, G. Bidoglio, Environ. Sci. Technol. 30 (1996) 598–604.
[7] Q.L. Yang, S.Z. Kang, H. Chen, W. Bu, J. Mu, Desalination 266 (2011) 149–153.
[8] G. Férey, Chem. Soc. Rev. 37 (2008) 191–214.
[9] C. Sanchez, B. Julian, P. Belleville, M. Popall, J. Mater. Chem. 15 (2005) 3559–3592.
[10] S. Kitagawa, R. Kitaura, S. Noro, Angew. Chem. Int. Ed. 43 (2004) 2334–2375.
[11] A.R. Millward, O.M. Yaghi, J. Am. Chem. Soc. 127 (2005) 17998–17999.
[12] B.V. Harbuzaru, A. Corma, F. Rey, P. Atienzar, J.L. Jordá, H. García, D. Ananias, L.D. Carlos, J. Rocha, Angew. Chem. Int. Ed. 47 (2008) 1080–1083.
[13] M. Vallet-Regi, F. Balas, D. Arcos, Angew. Chem. Int. Ed. 46 (2007) 7548–7558.
[14] C. Janiak, Dalton Trans. (2003) 2781–2804.
[15] D. Farrusseng, S. Aguado, C. Pinel, Angew. Chem. Int. Ed. 48 (2009) 7502–7513.
[16] A. Corma, H. García, F.X. Llabrés, i. Xamena, Chem. Rev. 110 (2010) 4606–4655.
[17] J. Lee, O.K. Farha, J. Roberts, K.A. Scheidt, S.T. Nguyen, J.T. Hupp, Chem. Soc. Rev. 38 (2009) 1450–1459.
[18] J. Long, S. Wang, Z. Ding, S. Wang, Y. Zhou, L. Huang, X. Wang, Chem. Commun. 48 (2012) 11656–11658.
[19] S.J. Garibay, S.M. Cohen, Chem. Commun. 46 (2010) 7700–7702.
[20] J. Gascon, M.D. Hernandez-Alonso, A.R. Almeida, G.P. van Klink, F. Kapteijn, G. Mul, ChemSusChem 1 (2008) 981–983.
[21] F. Vermoortele, M. Vandichel, B. Van de Voorde, R. Ameloot, M. Waroquier, V. Van Speybroeck, D.E. De Vos, Angew. Chem. Int. Ed. Engl. 51 (2012) 4887–4890.
[22] F.X. Llabrés i Xamena, A. Corma, H. García, J. Phys. Chem. C 111 (2006) 80–85.
[23] M. Alvaro, E. Carbonell, B. Ferrer, F.X. Llabres i Xamena, H. García, Chem. Eur. J. 13 (2007) 5106–5112.
[24] C. Gomes Silva, I. Luz, F.X. Llabrés i Xamena, A. Corma, H. García, Chem. Eur. J. 16 (2010) 11133–11138.
[25] Y. Fu, D. Sun, Y. Chen, R. Huang, Z. Ding, X. Fu, Z. Li, Angew. Chem. Int. Ed. 51 (2012) 3364–3367.
[26] Y. Horiuchi, T. Toyao, M. Saito, K. Mochizuki, M. Iwata, H. Higashimura, M. Anpo, M. Matsuoka, J. Phys. Chem. C 116 (2012) 20848–20853.
[27] T. Toyao, M. Saito, Y. Horiuchi, K. Mochizuki, M. Iwata, H. Higashimura, M. Matsuoka, Catal. Sci. Tech. 3 (2013) 2092–2097.
[28] L. Shen, L. Huang, S. Liang, R. Liang, N. Qin, L. Wu, RSC Adv. 4 (2014) 2546–2549.
[29] L. Shen, S. Liang, W. Wu, R. Liang, L. Wu, J. Mater. Chem. A 1 (2013) 11473–11482.
[30] L. Shen, W. Wu, R. Liang, R. Lin, L. Wu, Nanoscale 5 (2013) 9374–9382.
[31] L. Shen, S. Liang, W. Wu, R. Liang, L. Wu, Dalton Trans. 42 (2013) 13649–13657.

[32] C. Volkringer, M. Meddouri, T. Loiseau, N. Guillou, J. Marrot, G. Férey, M. Haouas, F. Taulelle, N. Audebrand, M. Latroche, Inorg. Chem. 47 (2008) 11892–11901.
[33] L. Wu, M. Xue, S.L. Qiu, G. Chaplais, A. Simon-Masseron, J. Patarin, Microporous Mesoporous Mater. 157 (2012) 75–81.
[34] A. Idris, N. Hassan, R. Rashid, A.F. Ngomsik, J. Hazard. Mater. 186 (2011) 629–635.
[35] M. Kurihara, H. Nishihara, Coord. Chem. Rev. 226 (2002) 125–135.
[36] V.W.W. Yam, C.C. Ko, N. Zhu, J. Am. Chem. Soc. 126 (2004) 12734–12735.
[37] V. Spagnol, E. Sutter, C. Debiemme-Chouvy, H. Cachet, B. Baroux, Electrochim. Acta 54 (2009) 1228–1232.
[38] A. Ishikawa, T. Takata, J.N. Kondo, M. Hara, H. Kobayashi, K. Domen, J. Am. Chem. Soc. 124 (2002) 13547–13553.
[39] X. Wang, S.O. Pehkonen, A.K. Ray, Ind. Eng. Chem. Res. 43 (2004) 1665–1672.
[40] C.R. Chenthamarakshan, H. Yang, Y. Ming, K. Rajeshwar, J. Electroanal. Chem. 494 (2000) 79–86.
[41] T. Tan, D. Beydoun, R. Amal, J. Photochem. Photobiol., A: Chem. 159 (2003) 273–280.
[42] J. Giménez, M.A. Aguado, S. Cervera-March, J. Mol. Catal. A 105 (1996) 67–78.